Ab initio calculations of electric-field-induced stress profiles for diamond/*c*-BN (110) superlattices

Shoji Ishibashi,[1] Tomoyuki Tamura,[1] Shingo Tanaka,[2] Masanori Kohyama,[2] and Kiyoyuki Terakura[1,3]
[1]*Research Institute for Computational Sciences (RICS), National Institute of Advanced Industrial Science and Technology (AIST), 1-1-1 Umezono, Tsukuba, Ibaraki 305-8568, Japan*
[2]*Research Institute for Ubiquitous Energy Devices (UBIQEN), AIST, 1-8-31 Midorigaoka, Ikeda, Osaka 563-8577, Japan*
[3]*Japan Advanced Institute of Science and Technology (JAIST), 1-1 Asahidai, Nomi, Ishikawa 923-1292, Japan*
(Received 5 May 2007; revised manuscript received 20 August 2007; published 23 October 2007)

We have investigated microscopic distributions of the electric-field-induced stress components for diamond/*c*-BN (110) superlattices with *ab initio* calculations. At zero electric field, tensile and compressive stresses exist for the diamond and BN layers, respectively, in the plane perpendicular to the stacking direction. Applying a static electric field, forces act on the B and N atoms and an apparent shear stress field appears in the BN layers. With atomic position relaxed, the shear stress extends to the whole region.

DOI: 10.1103/PhysRevB.76.153310 PACS number(s): 68.65.Cd, 71.15.−m, 73.21.Cd

Diamond and cubic boron nitride (*c*-BN) are promising wide-gap semiconductors because of their superiority in various properties such as high electrical and mechanical strengths, chemical inertness, and high thermal conductivity. In addition, they are excellent materials for low environmental load. Although preparing artificial structures for these materials is still a challenging task, they are expected to be in the mainstream for future electronic devices. Superlattices are one of the fundamental structures for applications. Several theoretical calculations have been performed to investigate stabilities and electronic properties of diamond/*c*-BN superlattices. Pickett[1] reported electronic structure calculations for diamond/*c*-BN (110) superlattices with 1+1, 3+3, and 5+5 layers in the unit cells. By investigating core levels and charges for constituent atoms, he concluded that three layers of each material are sufficient to give central layers whose core levels and charges are very close to those of the bulk. He also calculated valence-band and conduction-band discontinuities. Lambrecht and Segall[2] obtained similar results for the charge states of layers and the band discontinuities. In addition, they calculated formation energies of the superlattices and bonding properties at the interfaces.

In the present work, we have calculated stress profiles for diamond/*c*-BN (110) superlattices $(C_2)_{14-x}(BN)_x$ ($x=1,3,5,7,9,11,13$) and investigated effects of static electric field on them.

The calculations were carried out with our in-house computational code QMAS (quantum materials simulator),[3] which has been successfully applied in calculating, e.g., electronic structures of the organic conductor α-$(BEDT\text{-}TTF)_2I_3$,[4] Schottky barrier heights for metal/6*H*-SiC interfaces,[5,6] positron annihilation parameters in the Si system,[7] and dielectric properties of BN nanotubes.[8] We adopted the projector augmented-wave method.[9–11] As for the exchange and correlation energy for electrons, the generalized gradient approximation[12] was used together with the partial core correction.[13] The plane-wave cut-off energy was set to 20 hartree. For self-consistent calculations, $8\times8\times4$ $\boldsymbol{k}$ points were used in the full Brillouin zone. Structural optimization was made with convergence criteria of 5×10^{-5} hartree/bohr for forces on atoms and 5×10^{-7} hartree/bohr^3 for the sum of the stress components. Electronic structures under static electric field were calculated with the method proposed by Souza *et al.*[14] We performed self-consistent electronic structure calculations with electric field E between $\pm5\times10^{-3}$ a.u. along the stacking direction, where 5×10^{-3} a.u. corresponds to 0.257 V/Å. Stress densities were calculated with the method by Filippetti and Fiorentini.[15]

First, we worked on the 7+7 superlattice $[(C_2)_7(BN)_7]$ shown in Fig. 1. The stacking direction corresponds to the cubic [110] direction. Optimized lattice parameters and interlayer spacing values are listed in Table I. Each lattice parameter of the 7+7 superlattice has an intermediate value between those for diamond and BN. As for the interlayer spacing along the stacking direction, it is shown that those between the second and third planes from the interface almost recover bulk values. These are consistent with the previous results mentioned above.[1,2] Figure 2 represents the Born effective charges which have been evaluated with *ab initio* force calculations under the electric field.[14] The field was 5×10^{-3} a.u. (=0.257 V/Å). Note that BN is a polar material, while diamond is not polar. In the superlattice, however, C atoms at the interface are polar as shown in Fig. 2. It is also shown that B and N atoms located at the interface have distinct effective charges. For reference, Born effective charges for C in pure diamond and for B and N in cubic BN are 0, +1.92 and −1.92, respectively. In the superlattice, values for B and N atoms away from the interface have slightly larger magnitudes than those in cubic BN.

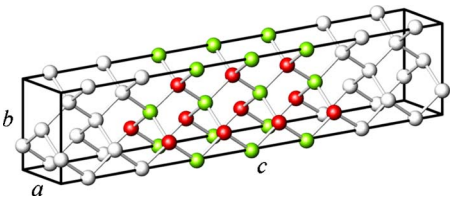

FIG. 1. (Color online) Crystal structure of the $(C_2)_7(BN)_7$ superlattice. C, B, and N atoms are represented with white, green (light gray), and red (dark gray) balls, respectively. The directions of the lattice vectors $\boldsymbol{a}$, $\boldsymbol{b}$, and $\boldsymbol{c}$ correspond to $[\bar{1}10]$, [001], and [110] directions of the original cubic lattice.

TABLE I. Optimized lattice parameters and interlayer spacing values along the stacking direction for $(C_2)_7(BN)_7$ (7+7). The values are given in Å. The interlayer spacing values are listed from those closer to the interface. Values for the bulk materials are also included for comparison. The cubic lattice constants for pure materials are listed in the b column. Those in parentheses in the a and c columns are $b/\sqrt{2}$ and $7b/\sqrt{2}$, respectively, which should be compared with a and c for the superlattice.

	a	b	c	$d_{C_2\text{-}C_2}$	$d_{BN\text{-}BN}$	$d_{C_2\text{-}BN}$
7+7	2.541	3.598	17.831	1.252	1.293	1.287
				1.262	1.277	
				1.261	1.283	
Bulk						
Diamond	(2.524)	3.569	(17.666)	1.262		
c-BN	(2.560)	3.621	(17.923)		1.280	

Figure 3 represents planar and macroscopic averages of stress profiles for $(C_2)_7(BN)_7$ at zero field. Each of them was obtained as follows. First, a set of stress-density values was calculated with the method by Filippetti and Fiorentini[15] on the three-dimensional mesh points set in the unit cell. Next, a planar averaged one-dimensional profile was obtained by summation along the x and y directions. Finally, the profile was microscopically averaged[16] by filtering it twice with specific lengths 1.261 and 1.283 Å, which are interlayer spacing values in the center regions of the diamond and BN layers given in Table I. This process is written as

$$\bar{\bar{\sigma}}_{ij}(z) = \frac{1}{d_1 d_2} \int_{z-d_1/2}^{z+d_1/2} dz_1 \int_{z_1-d_2/2}^{z_1+d_2/2} dz_2 \bar{\sigma}_{ij}(z_2), \qquad (1)$$

where $\bar{\sigma}_{ij}$ is the planar averaged profile and $\bar{\bar{\sigma}}_{ij}$ is the microscopically averaged one. There is a gauge-variance problem in describing the kinetic-energy term of the stress density as discussed by Filippetti and Fiorentini[15] as well as by Rogers and Rappe.[17] The last process is expected to average out small ambiguity[17] of the kinetic-energy term of the stress density in addition to eliminating sharp atomic oscillations.

From the variations of $\bar{\bar{\sigma}}_{11}$ and $\bar{\bar{\sigma}}_{22}$ in Fig. 3, it is obvious that tensile and compressive stresses exist in the ab planes of diamond and BN layers, respectively. This is quite natural considering the lattice parameters for the bulk materials and

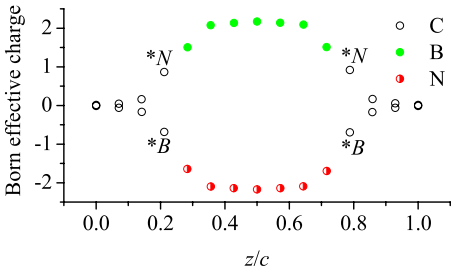

FIG. 2. (Color online) Born effective charge for the $(C_2)_7(BN)_7$ superlattice. "*B" or "*N" means that the C atom is bound with a B or N atom.

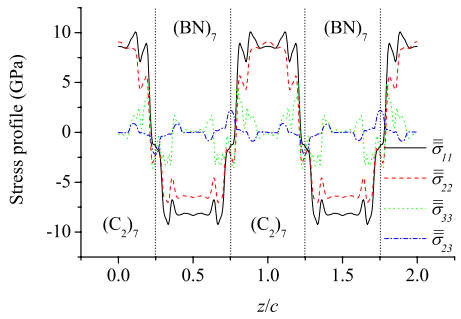

FIG. 3. (Color online) Stress profiles for $(C_2)_7(BN)_7$ at zero field. The center planes of diamond are located at $z=0.0, 1.0, 2.0$, while those of BN are located at $z=0.5, 1.5$. The vertical dotted lines represent the positions of interfaces.

the superlattice (they are shown in Table I). In contrast to the in-plane stress components, the stress along the stacking direction ($\bar{\bar{\sigma}}_{33}$) shows large relaxation. The reason is thought to be that atomic positions are able to be rearranged along this direction. As was already pointed out in Table I, the interlayer spacing in the c direction is essentially the same as that of the bulk material in the central part of each layer. This is the reason why the shear stress component $\bar{\bar{\sigma}}_{23}$ shows significant amplitudes only around the interfaces. At the interface, there are two kinds of bonds. The C-B bond length (1.61 Å) is longer than the C-N bond length (1.53 Å). This is the origin of the shear stress at the interface. It should also be mentioned that the stress values at the center parts of the diamond and BN layers are in good agreement with the macroscopic stress values for pure materials whose local structures are the same as the center parts of the layers.

Electric field causes not only electronic response but also mechanical ones through electrostriction. As already mentioned in the description of Fig. 2, the electric field causes significant forces on the polar atoms (B and N atoms as well as C atoms at the interface). We calculated stress profiles also at the instant of applying the field of 5×10^{-3} a.u. (=0.257 V/Å) along the c direction. The results are shown in Fig. 4 as the differences from those at zero field. The diago-

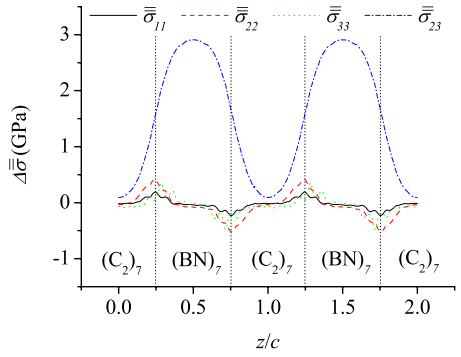

FIG. 4. (Color online) The differences between stress profiles for $(C_2)_7(BN)_7$ at zero field and those at the instant of applying the field (5×10^{-3} a.u.=0.257 V/Å). The center planes of diamond are located at $z=0.0, 1.0, 2.0$, while those of BN are located at $z=0.5, 1.5$.

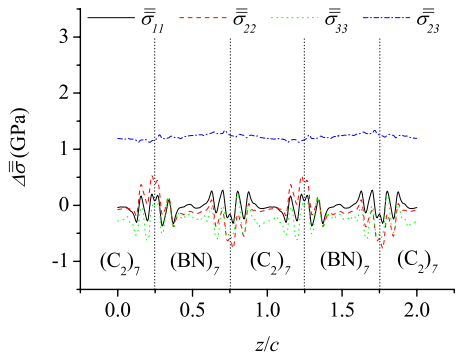

FIG. 5. (Color online) The differences between stress profiles for $(C_2)_7(BN)_7$ at zero field and those under finite field (5×10^{-3} a.u.$=0.257$ V/Å) with atomic positions fully relaxed. The center planes of diamond are located at $z=0.0, 1.0, 2.0$, while those of BN are located at $z=0.5, 1.5$.

nal components of the stress tensor seem not to show any significant changes, while the shear stress component $\bar{\bar{\sigma}}_{23}$ emerges preferentially in the BN region. The $\bar{\bar{\sigma}}_{23}$ profile can be related to the Born effective charge distribution in Fig. 2, since both reflect induced forces on the polar atoms by the electric field.

Since significant forces act on some atoms under the field, we made atomic position optimization. After the optimization, the stress profiles were calculated again and the differences from those at zero field are plotted in Fig. 5. It is shown that the shear stress extends to the whole region and the $\bar{\bar{\sigma}}_{23}$ value is almost constant. As for space-averaged shear stress values (σ_{23}) before and after atomic position optimization, we have investigated their dependence on the electric field strength (E). The ratio of σ_{23} to E is plotted as a function of E in Fig. 6. Those before optimization are almost constant. In contrast with this, those after optimizations show a nonlinear behavior. For the latter case, the ratio of σ_{23} to E increases with $|E|$ increasing. We have found that the ratio of the averaged atomic displacement to E shows a similar behavior. Anharmonicity in atomic displacements under the electric field is thought to be the origin of the nonlinearity. By fitting the relation between σ_{23} and E to cubic polynomials, we evaluated linear coefficients (a_1) and third-order coefficients (a_3) with significant amplitudes. For before and

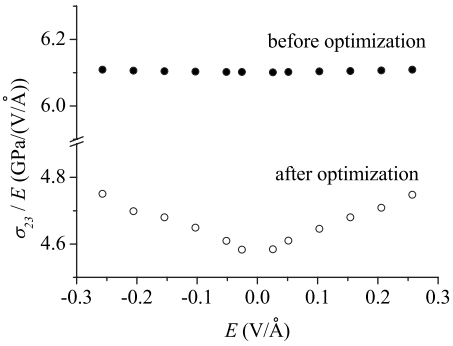

FIG. 6. Ratio of space-averaged shear stress value σ_{23} to electric field E for $(C_2)_7(BN)_7$.

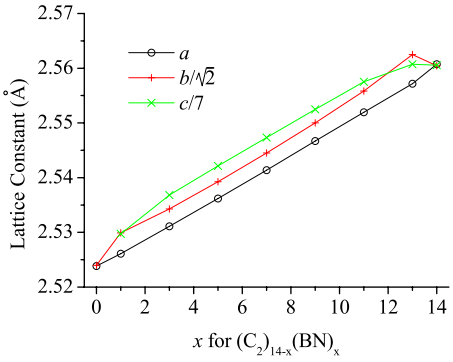

FIG. 7. (Color online) Lattice parameter variation for the $(C_2)_{14-x}(BN)_x$ superlattice.

after optimization, $a_1=6.1023\pm0.0001$ GPa/(V/Å) and 4.628 ± 0.005 GPa/(V/Å) and $a_3=0.103\pm0.003$ GPa/(V/Å)^3 and 1.8 ± 0.1 GPa/(V/Å)^3.

In the following, results for the superlattice with various compositions $(C_2)_{14-x}(BN)_x$ ($x=1,3,5,7,9,11,13$) are shown. Lattice parameters and atomic positions were fully optimized with *ab initio* calculations. The resultant lattice parameters are plotted in Fig. 7 together with those for pure diamond (denoted as $x=0$) and pure c-BN ($x=14$). The lattice parameter a shows a linear dependence in the whole x range, while b and c show nonlinear changes between $x=0$ and $x=1$ as well as between $x=13$ and $x=14$. Fractional coordinates of the atomic positions can take only 0 or 0.5 along a by symmetry, while they can relax along b or c. In fact, significant atomic relaxations are observed in the vicinity of the interface along these directions. In other words, among four bonds that one atom contributes, two bonds are fixed within the bc plane, while the other two bonds have more flexibility. As for the c direction, there is a straightforward evidence in Table I. The difference between $d_{\text{C2-BN}}\times2$ (there are two interfaces) and $d_{\text{C2-C2}}+d_{\text{BN-BN}}$ for pure materials is 0.032 Å. This expansion of interlayer distance at the interface contributes to the average lattice constant $c/7$ by about 0.005 Å, which is the major part of the additional lattice constant expansion along c in Fig. 7. Details of the interface structure will be reported elsewhere related to mechanical properties. In the following, we focus on electric field effects on stress profiles for the superlattices with various compositions.

The stress component profiles were calculated with a slightly different way from that used for the 7+7 superlattice ($x=7$). For small x (=1,3) or large x (=11,13), it is difficult to set one of two specific lengths to obtain macroscopic averages with Eq. (1). The macroscopic averaging is equivalent to double convolutions with two rectangular window functions. Instead, we used a Gaussian window function with a full width at half maximum (FWHM) of 2.0 Å to broaden profiles. The FWHM value was determined as a minimal value to eliminate sharp atomic oscillations. The stress profiles obtained in this way for $x=7$ (not shown) are quite similar to those shown in Fig. 3. For all x (=1,3,5,7,9,11,13), tensile in-plane stresses exist in the diamond layer, while compressive in-plane stresses exist in the BN layer.

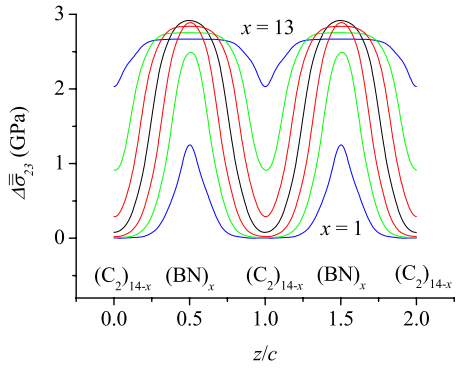

FIG. 8. (Color online) The differences between stress profiles for $(C_2)_{1-x}(BN)_x$ at zero field and those at the instant of applying the field (5×10^{-3} a.u.=0.257 V/Å). The center planes of diamond are located at z=0.0, 1.0, 2.0, while those of BN are located at z =0.5, 1.5.

With the same Gaussian window function, we calculated the $\bar{\bar{\sigma}}_{23}$ profiles at the instant of applying the field of 5×10^{-3} a.u. (=0.257 V/Å). The differences from the zero-field values are shown in Fig. 8. A systematic variation reflecting the superlattice periodicity is observed. Again, the shear stress emerges preferentially in the BN region. The results after atomic relaxation are shown in Fig. 9. The shear stress extends to the whole region and each profile is fairly independent of the position z similar to the result in Fig. 5. The magnitude of $\bar{\bar{\sigma}}_{23}$ is roughly proportional to the BN composition x. Note that the results for x=7 shown in Figs. 8 and 9 are very similar to those in Figs. 4 and 5. This justifies the use of the Gaussian window function.

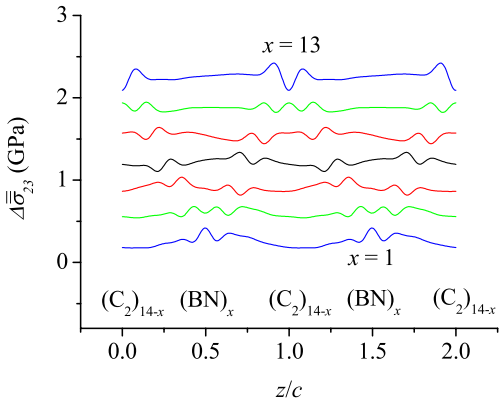

FIG. 9. (Color online) The differences between stress profiles for $(C_2)_{1-x}(BN)_x$ at zero field and those under finite field (5×10^{-3} a.u.=0.257 V/Å) with atomic positions fully relaxed. The center planes of diamond are located at z=0.0, 1.0, 2.0, while those of BN are located at z=0.5, 1.5.

In summary, we have calculated electric-field-induced stress profiles for the diamond/BN (110) superlattices with *ab initio* methods. The computational scheme shown in the present work is expected to be useful for studying electromechanical effects in electronic devices, microelectromechanical systems, and so on.

This work was partly supported by the Next Generation Super Computing Project, Nanoscience Program, MEXT, Japan.

[1] W. E. Pickett, Phys. Rev. B **38**, 1316 (1988).
[2] W. R. L. Lambrecht and B. Segall, Phys. Rev. B **40**, 9909 (1989).
[3] S. Ishibashi, T. Tamura, S. Tanaka, M. Kohyama, and K. Terakura (unpublished).
[4] S. Ishibashi, T. Tamura, M. Kohyama, and K. Terakura, J. Phys. Soc. Jpn. **75**, 015005 (2006).
[5] S. Tanaka, T. Tamura, K. Okazaki, S. Ishibashi, and M. Kohyama, Mater. Trans. **47**, 2690 (2006).
[6] S. Tanaka, T. Tamura, K. Okazaki, S. Ishibashi, and M. Kohyama, Phys. Status Solidi C **4**, 2972 (2007).
[7] A. Uedono *et al.*, J. Appl. Phys. **100**, 034509 (2006).
[8] G. Y. Guo, S. Ishibashi, T. Tamura, and K. Terakura, Phys. Rev. B **75**, 245403 (2007).
[9] P. E. Blöchl, Phys. Rev. B **50**, 17953 (1994).
[10] N. A. W. Holzwarth, G. E. Matthews, R. B. Dunning, A. R. Tackett, and Y. Zeng, Phys. Rev. B **55**, 2005 (1997).
[11] G. Kresse and D. Joubert, Phys. Rev. B **59**, 1758 (1999).
[12] J. P. Perdew, K. Burke, and M. Ernzerhof, Phys. Rev. Lett. **77**, 3865 (1996).
[13] S. G. Louie, S. Froyen, and M. L. Cohen, Phys. Rev. B **26**, 1738 (1982).
[14] I. Souza, J. Íñiguez, and D. Vanderbilt, Phys. Rev. Lett. **89**, 117602 (2002).
[15] A. Filippetti and V. Fiorentini, Phys. Rev. B **61**, 08433 (2000).
[16] A. Baldereschi, S. Baroni, and R. Resta, Phys. Rev. Lett. **61**, 734 (1988).
[17] C. L. Rogers and A. M. Rappe, Phys. Rev. B **65**, 224117 (2002).